Eksploatacja i Niezawodnosc – Maintenance and Reliability
Volume 22 (2020), Issue 4
journal homepage: http://www.ein.org.pl

Article citation info:
Li Y-H, Liang X-J, Dong S-H. Reliability optimization design method based on multi-level surrogate model. Eksploatacja i Niezawodnosc – Maintenance and Reliability 2020; 22 (4): 638–650, http://dx.doi.org/10.17531/ein.2020.4.7.

Reliability optimization design method based on multi-level surrogate model

Indexed by: Web of Science Group

Yong-Hua Li [a*], Xiao-Jia Liang [b], Si-Hui Dong [c]

[a]School of Locomotive and Rolling Stock Engineering, Dalian Jiaotong University, Liaoning, 116028, P.R. China
[b]CRRC Changchun Railway Vehicle Co., Ltd, Jilin, 130062, P. R. China
[c]School of Traffic and Transportation Engineering, Dalian Jiaotong University, Liaoning, 116028, P.R. China

Highlights

- A multi-point addition criterion of genetic-algorithm-based is introduced to the Kriging model.
- A multi-level surrogate model is first proposed considering the poor local search performance of Kriging model.
- A design optimization approach combined multi-level surrogate model with reliability is studied.

Abstract

In this work, a genetic-algorithm-based Kriging model with multi-point addition sequence optimization strategy is addressed to make up for the shortcomings of Kriging model with single point criterion. This approach combines the multi-point addition strategy with genetic algorithm to enable the Kriging model to efficiently capture the globally optimal solution. Based on this, a multi-level surrogate method is presented by employing a local surrogate model to modify the Kriging global surrogate model, and then applied to design optimization to improve the accuracy and efficiency of global optimization. Meanwhile, a reliability design optimization method based on multi-level surrogate model is studied by dealing with the reliability constraints with an adaptive reliability penalty function. Numerical examples show that the proposed method can find the optimal solution of the object problem with the least calculation cost under the condition of satisfying the reliability constraint.

Keywords

Kriging model, reliability-based optimization, multi-level surrogate model, adaptive dynamic penalty function.

Acronyms and Abbreviations

RBDO	Reliability-based design optimization
RBF	Radial basis function
QP	Quadratic polynomial
PQP	Perfect quadratic polynomial
RMSE	Root mean square error

Notations

ξ	Regression coefficient
$F(x)$	Polynomial matrix of x
$R(\theta, x_i, x_j)$	Spatial correlation between training samples
$\hat{\sigma}^{2(k)}(x_i)$	Prediction of variance in kth iteration of any sample.
$\hat{\sigma}^{2(k)}_{\max}$	Maximum prediction of variance in k-th iteration.
λ	Proportional control factor.
$\hat{f}^{(k)}_{\min}$	Prediction of optimal design in k-th iteration.
$f^{(k)}_{\min}$	Finite element value of optimal design in kth iteration.
ε	Precision.
d	Euclidean metric.
p_c	Operator of selective probability.
p_m	Operator of mutation probability.
j	Number of structural function
$g_j(x)$	The jth structural function.
$P[g_j(x) > 0]$	Probability of reliability of jth structural function.
$[P_r]$	Allowable probability of reliability.
$[\beta_j(x)]$	Reliability index of j-th structural function.
$[\beta]$	Allowable reliability index
$f(x)$	Objective function.
$p(x)$	Penalty function.
$\tilde{f}(x)$	Objective satisfaction function.
$\tilde{p}(x)$	Constraint satisfaction function.
ρ	Proportion of feasible solution.
t	Number of iterations.
α	Adjustable factor.
$r(\rho)$	Adaptive dynamic penalty factor.

(*) Corresponding author.
E-mail addresses: Y-H Li - liyh@djtu.edu.cn, X-J Liang - 013200029892@crrcgc.cc, S-H Dong - shdong@djtu.edu.cn

1. Introduction

With the development of research in the field of structural reliability in China, the application of reliability-based design optimization (RBDO) has become increasingly prominent. RBDO can give a more secure and reliable design scheme than traditional design optimization methods while fully considering the random uncertainty of design parameters. This optimization method can improve the accuracy of the optimization results and obtain obvious economic benefits [17, 2, 31]. Therefore, there is a great significance to study the RBDO and its application.

Uncertainty exists at any stage in the design, manufacture, and operation of engineering systems [26, 15, 16]. Guaranteeing the reliability of the system under uncertainty is an important issue that needs to be concerned in RBDO. The surrogate model technology is applied to construct the performance function or optimize objective function under the approximate reliability constraints. This technology can reduce the computation cost and improve the efficiency of the design optimization. Aiming at this research field, Yu et al. [28] used the quadratic polynomial response surface (PRS) model to establish an approximate performance function model of the wing structure, and the RBDO model as the constraint function is established by using the reliability of the maximum stress and the maximum displacement. The fmincon function in the MATLAB optimization toolbox is applied to solve the lightweight problem of the wing structure. Ozcanan et al. [23] used radial basis function (RBF)-based metamodels of the roadside safety equipment based on data obtained by the crash test simulation and the RBF approximation model is optimized by using the multi-objective genetic algorithm. Zhou et al. [32] proposed an improved quadratic PRS model to replace the performance function of the ablation life of fast-fire weapon, and finished the RBDO of the body tube ablation life. Bahman et al. [1] proposed a four-bar mechanisms optimization method based on game theory and data processing artificial neural network (ANN) grouping method which is also utilized to construct an approximate model for the rational reaction set of the followers, and the mechanism optimization is realized by adopting the neural network. Zhang et al. [30] proposed a design idea of combining Kriging model with first-order reliability calculation method. The optimal results are successfully obtained when they applied it to reliability-based crashworthiness design optimization research of aluminum foam filled structure. Although PRS, PBF, ANN and Kriging models can be used to express the functional relationship between optimization variables and their responses, they all have some shortcomings. PRS is the only explicit surrogate model, which can not only accurately obtain the functional relationship between the optimization variables and the response values, but also facilitate the optimization by using the optimization algorithm. However, the fitting accuracy of strong nonlinear function is poor. RBF, ANN and Kriging have high fitting accuracy for functions with high nonlinear, but it is easy to fall into local optimal solution and difficulty in convergence. Among these methods, in view of Kriging model has the advantages of improving the quantitative evaluation accuracy of prediction model and the few modeling parameters, this paper improves the traditional model in order to improve the accuracy of RBDO.

To this end, a multi-point addition strategy based on a Kriging surrogate model and RBDO method based on multi-level surrogate model are proposed after he objective function optimization and reliability constraints is deeply analyzed. The efficiency of the method is next verified by some cases. The rests of this study are organized as follows: the traditional Kriging model is introduced in section 2. Following this, section 3 proposed a genetic-algorithm-based Kriging surrogate model using multi-point addition sequence optimization strategy and section 4 presented multi-level objective surrogate optimization method. A multi-level surrogate model based reliability design optimization method is studied in section 5. Finally, conclusions are given in section 6.

2. Kriging Surrogate Model

Kriging surrogate model is a kind of local interpolation method to estimate the unbiased optimal value of variables in a limited area. It predicts at a certain point depends on the information of known variables around this point, that is, the unknown information of this point is estimated by the linear combination of weighted information within a certain range of this point [12, 22, 21]. Thus, it is also called optimal linear unbiased estimation and the mathematical function of Kriging surrogate model is expressed as an equation, the equation can be given by:

$$\tilde{y}(x) = F(\xi, x) + z(x) = f(x)^T \xi + z(x) \tag{1}$$

where ξ is the regression coefficient; $F(x)$ is the polynomial matrix of x; $z(x)$ is the error of spatial correlation random distribution, and its covariance can be provided by:

$$\mathrm{cov}[z(x_i), z(x_j)] = \sigma_z^2 [R(\theta, x_i, x_j)] \tag{2}$$

where x_i and x_j are any two points in the training samples; σ_z^2 is the variance of randomly distributed errors; $R(\theta, x_i, x_j)$ is the spatial correlation between training samples, which is expressed as follows:

$$R(\theta, x_i, x_j) = \prod_{k=1}^{m} R_k(\theta_k, d_k), \; d_k = \left| x_i^k - x_j^k \right| \tag{3}$$

3. Genetic-algorithm-based kriging surrogate model using multi-point addition sequence optimization strategy

3.1. Kriging-based sequence optimization

The Kriging surrogate model has good global approximation ability. Using Kriging surrogate model to fit the objective function of structural performance can better reflect the real model functional relationship. Common optimization methods of Kriging surrogate model include "one-step" design optimization and sequence iterative optimization design [33, 8].

The "one-step" design optimization is a method of selecting a certain number of training samples in the design variable space through the experimental design method. The Kriging surrogate model is constructed by using the training samples and their response values. And then perform the accuracy test on the model. The directly design optimization is applied on the Kriging surrogate model when the model meets the accuracy requirements.

Sequence iterative design optimization is a method that considers the prediction uncertainty and predicted values to increase the sample and improve the fitting accuracy of the model to perform sequence iterative optimization [18, 34, 5]. The optimization process is shown in Fig. 1. The second method achieves the purpose of improving the fitting accuracy of the Kriging model and the accuracy of the optimization result in the sequence iterative process. Compared with the Kriging model in the one-step optimization design, the sequence iterative optimization design reduces the dependence on the initial sample.

3.2. Kriging-based multi-point addition criterion

Kriging surrogate model is an interpolation approximation method. It can not only give the response value of the predicted point, but also give the variance of the predicted value. If there are few number of sample points in the region near a predicted point, the variance

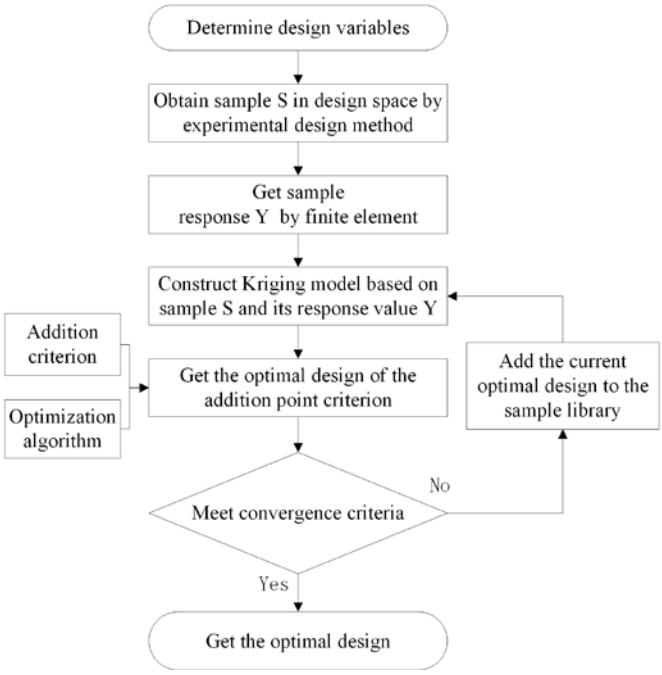

Fig. 1. The flow chart of sequential optimization based on Kriging model

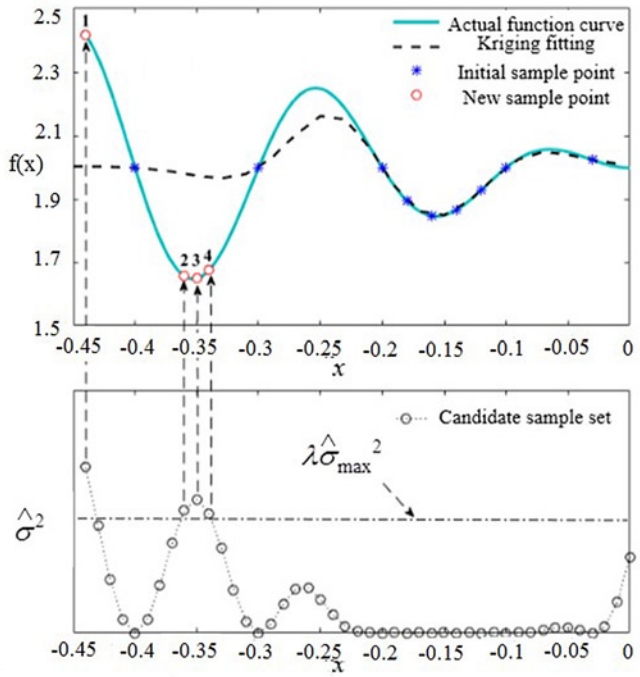

Fig. 2. Infill criteria based on Kriging prediction

obtained by calculating the prediction point through Kriging model is large. This variance carries the uncertainty information of the predicted point, or it can be considered that the sample near the point is sparse. If the variance of the predicted points is large, the uncertainty of the predicted values is higher [24, 9]. Therefore, in the view of the shortcomings of the above single-point criterion, this paper proposes a multi-point addition criterion based on the Kriging surrogate model. In other words, adding some sample points near the prediction point to improve the fitting accuracy of the model. The adding point criterion can not only keep the current optimal design and explore the areas with large uncertainties, but also can capture the change trend of the optimization target in time under current optimal design.

"Multi-point addition" refers to adding several new sample points in each sequence iterative optimization process. The new sample library contains the initial sample points, the current optimal design points, and the points with larger variances of Kriging prediction values. The current optimal design point is similar to the optimal insertion criterion that is obtained by the Kriging-based optimization algorithm to preserve the optimal design result of each iteration, especially to prevent the loss of global information when the current optimal design point is close to the real globally optimal points [11, 20]. Regarding the selection method of the larger prediction variance, firstly the candidate sample set of the selected points is generated in the design space. And then the variance of the corresponding predicted value is calculated according to the current Kriging surrogate model. If the prediction variance of a certain point is greater than the predetermined threshold, the point is treated as a point with the large variance. Otherwise, the point is discarded. The prediction variance can be described as follows:

$$\hat{\sigma}^{2(k)}(x_i) > \lambda \hat{\sigma}^{2(k)}_{\max}, \ k = 1,2,...,\mathrm{n} \tag{4}$$

where x_i is any sample point in the given candidate sample set; $\hat{\sigma}^{2(k)}_{\max}$ is the maximum prediction variance in the candidate sample set at the k-th iteration; λ is a selection ratio control factor. The value of λ determines the number of new points.

Fig. 2 is a schematic diagram of selecting the larger variance. The black hollow points in the Fig. 2 constitute the candidate sample set in the design space. The new sample points are selected by comparing the calculated variance of the predicted value with the predetermined threshold. The point newly added is the design point corresponding to the four black hollow points above the dotted line in the Fig. 2, where the arrow points to the position in the actual function curve and is marked as a red hollow point. If the value of λ is large, the dotted line moves up, so the number of points that can be selected will decrease. Otherwise, the number of points will increase. In addition, it can be seen from Fig. 2 that the four new sample points fill well with the regions that the initial samples are not covered, and optimization algorithm is guided to search in the region with lacking the sample information. Point 1 is located near the region with the highest uncertainty. Adding point 1 indicates that the iteration is performing a global search; if point 3 is considered to be the current optimal design point, points 2 and 4 are located near the current optimal design point. Adding points 2 and 4 indicates that the iteration is performing a local search.

3.3. Genetic-algorithm-based Kriging model using multi-point addition sequence optimization strategy

The optimization algorithm is crucial in the sequence iterative optimization. Under the premise of a certain kind of point addition criterion, it can search for the update points needed for the surrogate model reconstruction during the iterative process, which can improve the fitting accuracy of the surrogate model. In the sequence optimization of the Kriging surrogate model, the optimization target is to construct surrogate model by Kriging interpolation technique. Compared with the actual engineering simulation model, the time cost for optimization is greatly reduced by the optimization algorithm of surrogate model. In the view of the powerfully global search capability of genetic algorithm, the process is much simple without too many mathematical requirements [27, 7]. Therefore, the genetic algorithm is applied to optimization based on sections 3.1 and 3.2. The optimization design process is shown in Fig. 3, and the steps are as follows:

1) Select the encoding method to generate the initial population P(t).
2) The initial training sample is generated in the design space by uniform design, and the real response value of the sample is obtained through finite element analysis of structure.

3) Establish a Kriging surrogate model for the objective function of the RBDO.
4) The fitness value (objective function value) of each individual in the population can be get by the Kriging prediction.
5) Form the progeny population P(t+1) by selecting, intersecting, and mutating on the individuals in the population. And select the optimal individuals according to the order of fitness.
6) Obtain the current optimal individual as well as the real model response value of optimal design point through the finite element analysis.
7) Determine whether the convergence criterion is met. If the convergence criterion is met, stop the optimization and get the optimal design; otherwise, put the current optimal design into the sample set and turn to the next step. The two convergence criteria which are used as follows:

$$\left|\frac{\hat{f}_{\min}^{(k)} - \hat{f}_{\min}^{(k-1)}}{\hat{f}_{\min}^{(k-1)}}\right| \le \varepsilon \tag{5}$$

$$\left|\frac{\hat{f}_{\min}^{(k)} - f_{\min}^{(k-1)}}{f_{\min}^{(k-1)}}\right| \le \varepsilon \tag{6}$$

where ε usually equates 0.001; $f^{(k)}$ and $\hat{f}^{(k)}$ respectively represent the finite element analysis values of the k-th iteration optimization and the Kriging surrogate model prediction values of the *k*-th iteration optimization.

Eq. (5) is the accuracy requirement for the optimal solution, and Eq. (6) is the global requirement for the optimal solution. Meeting both two convergence criteria at the same time can ensure that the optimal solution is the globally accurate optimal solution. Eq. (6) can be used directly when the global requirements for the optimal solution are not too high.

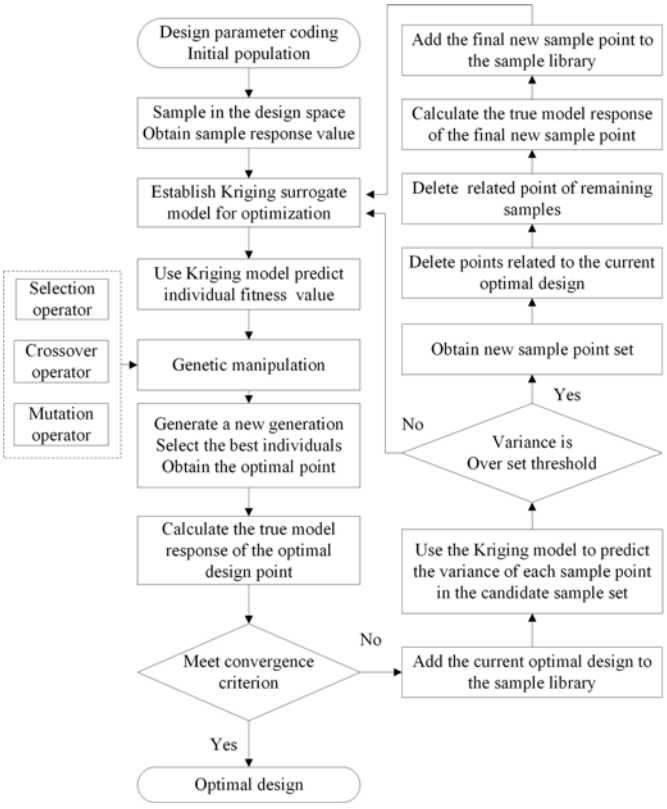

Fig. 3. Optimization flowchart for multi-point addition criterion of Kriging model based on genetic algorithm

8) Use the MC method to generate the candidate sample set in the design space, and determine whether the prediction variance of each sample by Kriging exceeds the set threshold $\lambda\hat{\sigma}^{2(k)}$. If the maximum value of the predicted variance does not exceed the threshold, then directly return to step (3); otherwise, the sample points whose predicted variance exceeds the threshold are regarded as points with larger variance, and the larger points of these variances constitute the initial set of newly added samples. Then delete the related point and leave the unrelated points to the sample library. Return to step (3) until the convergence criterion is met.

3.4. Numerical cases analysis

The common test function is used to analyze the effects of the initial λ and the candidate sample sets d on the optimization results. These two parameters determine the number of newly added samples, where the parameters λ control the number of initial new samples, and the value is set to $[0.5, 0.6, 0.7, 0.8, 0.9]$; the parameter d involves the deletion of the information related point, which is set to $[0.001, 0.005, 0.01, 0.1, 0.5]$. The $5n(n = 1,2,...,6)$ uniform design is adapted to select the initial sample, and the number of candidate sample sets produced by MC method is $25n(n = 1,2,...,5)$.

The main analysis is about how different parameters combinations and the number of initial samples and candidate sample influence the optimization efficiency and the optimal solution accuracy. During the analysis, the evaluation criterion of the optimization efficiency is the number of original function operations N_S. The accuracy evaluation involves relative error, absolute error and root mean square error (RMSE). Table 1 gives related parameter settings.

The Ackley's Path function is superimposed by the enlarged cosine function and the exponential function. The specific expression is as follows:

$$\text{Min } f = -20e^{-0.2\sqrt{\sum_{i=1}^{m} x_i^2/m}} - e^{\sqrt{\sum_{i=1}^{m} \cos(2\pi x_i)/m}} + 20 + e \tag{7}$$

where m is variable dimension. When $m = 2$, variable value range: $-2 \le x_1, x_2 \le 2$.

Table 1. Parameter setting

Parameter	Setting
Initial population	50
Selection probability p_c	0.95
Mutation probability p_m	0.001
ε	0.001

Ackley's Path function is shown in Fig. 4. It can be seen from Fig. 4(a) that the Ackley's Path function is a multi-peak, multi-extreme function, and the gradient at the peak is larger. But it is difficult to capture the trend of the function value using the gradient optimization algorithm. There is a globally optimal solution $f(0,0,...,0) = 0$ of the optimization problem, as shown by the five-pointed asterisk in Fig. 4(b). It can be seen that there are eight locally optimal solutions near the optimal solution, marked as "*". And as the range of variable values expands, the number of local optimal solutions increases accordingly.

Uniform design is a deterministic experimental design, and the only thing that is known for sure is that the initial training sample is generated by the uniform design. Due to the randomness of the MC

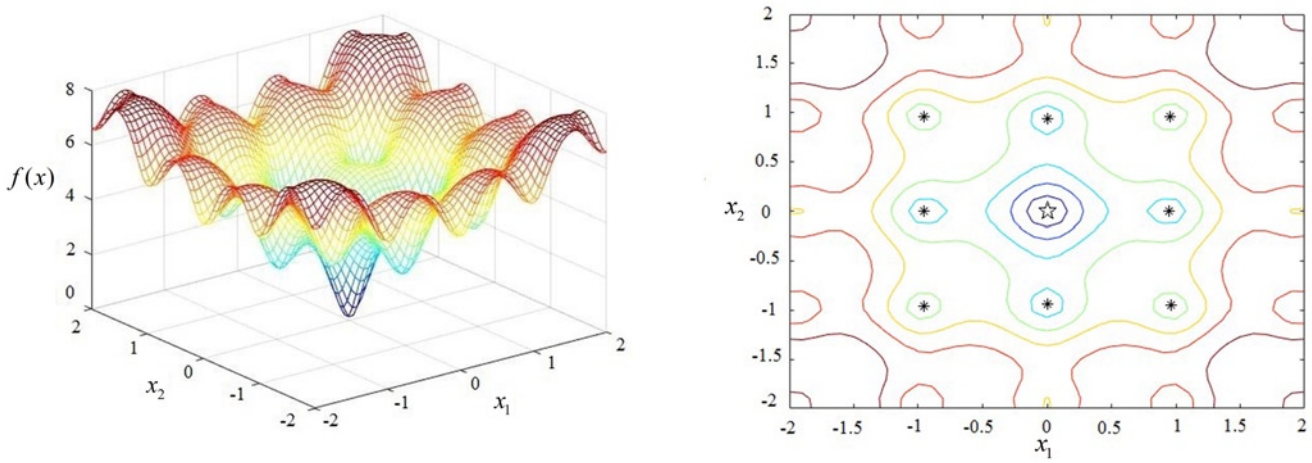

(a) Surface graph of Ackley's Path *(b) Contour plot of Ackley's Path*

Fig. 4. Ackley's Path test function

Table 2. Optimization results under different initial sample numbers

Uniform design	N_S	Worst	Optimal	Average	Standard deviation	Absolute error	RMSE
5P	63	0.523	0.023	0.028	0.026	0.028	0.455
10P	65	0.197	0.017	0.023	0.017	0.023	0.212
15P	66	0.068	0.004	0.020	0.022	0.020	0.039
20P	66	0.059	0.003	0.016	0.018	0.016	0.033
25P	68	0.062	0.003	0.012	0.011	0.012	0.056
30P	71	0.055	0.003	0.012	0.013	0.012	0.062

method, the generated candidate sample may be good or bad, which will bring randomness to the optimization results [6]. In order to avoid the randomness, 50 groups of random optimization designs are performed, and the average value of these 50 groups is selected as the final result. In addition, in order to analyze the effect of the parameter settings optimization results, the results corresponding to the number of the different initial sample and the candidate sample are averaged. Meanwhile, the results corresponding to the different parameter combinations are averaged to analyze the results of the number of initial sample and the number of candidate sample sets on the optimization results. Since the globally optimal value is zero, the absolute error is applied instead of the relative error in the analysis for accuracy evaluation.

Table 2 shows the optimal solutions obtained by running the optimization designs 50 times with different initial sample numbers. It can be seen from the table that with the increase of the number of initial samples, the running number of the original function increases slightly, but the amplitude of increase is not obvious, and the average value of the optimization results is continuously increasing. When the number of initial sample is increased to 15, the optimal value, absolute error and RMSE have a significant reduction trend, and there is only little effect when continue to increase the number of sample. The standard deviation does not show obvious changes and it is generally at a lower level, which indicates that the optimization method is less dependent on the initial sample.

The 50 groups of optimal solutions with different numbers of the candidate sample groups are counted to obtain box plots of absolute error and root mean square error, and it is shown in Fig. 5 and Fig. 6. The shorter length of the rectangular box indicates that the data distribution is more concentrated and has strong robustness (weak dependence for the number of the candidate sample groups). The red horizontal line in the box represents the mean value. The closer to zero, the more accurate the optimization result is. Considering the overall trend, as the number of the candidate sample groups increases, the accuracy is continuously improving. When the number of the candidate sample groups gets to 100, the optimization result tends to be stable.

Fig. 7 and Fig. 8 show the number of the original function applications N_S and the absolute error of the optimization result for different parameter settings. It can be seen that the value of N_S increases with the value of λ increases and decreases with the value of d increases. If the value of λ is larger, the number of initial new sample points will be reduced after the larger variance judgment predicted by Kriging surrogate model. If the value of d is larger, the range of the correlation determination fields will be expanded, and the number of the points falling into the decision domain will increase. Thus, the smaller value of λ and d will reduce the number of new sample and function runs.

For the accuracy of optimization results, the smaller the λ, the higher the accuracy from the overall trend, which means that the smaller λ the more number of points can be put into the sample library, so that the fitting accuracy of the Kriging surrogate model can be improved to make optimization result closer to the globally optimal solution of the real function. In addition, when the different value of λ is taken, the influence trend of d is different. When the $\lambda < 0.7$, the influence of d on accuracy is little, while when the $\lambda \geq 0.7$, the influence of d on accuracy is much larger, but has no rules to follow. If the requirement of the globally optimal solution is not very high, the λ can be taken as 0.7 to ensure the accuracy and reduce the number of function runs and improve efficiency.

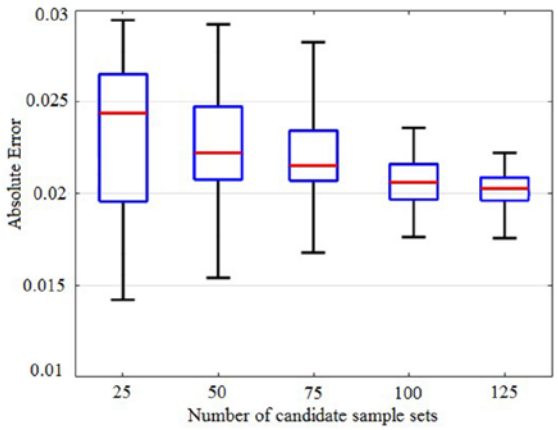

Fig. 5. Boxplot of absolute error

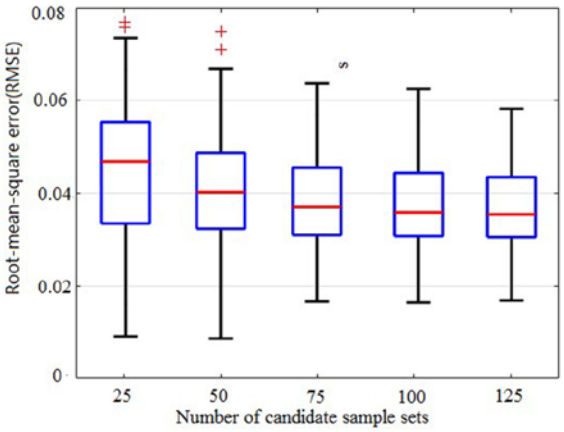

Fig. 6. Boxplot of RMSE

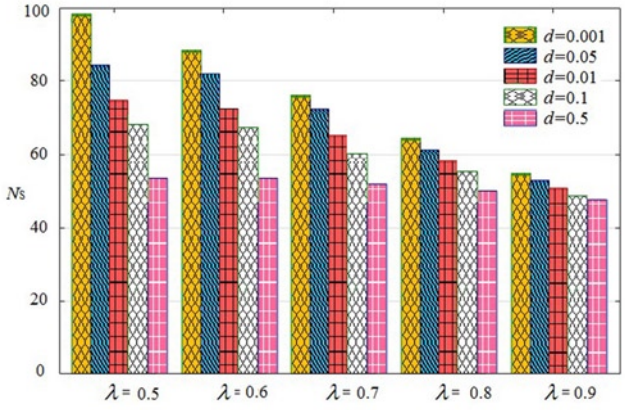

Fig. 7. The number of function running under different parameter combinations

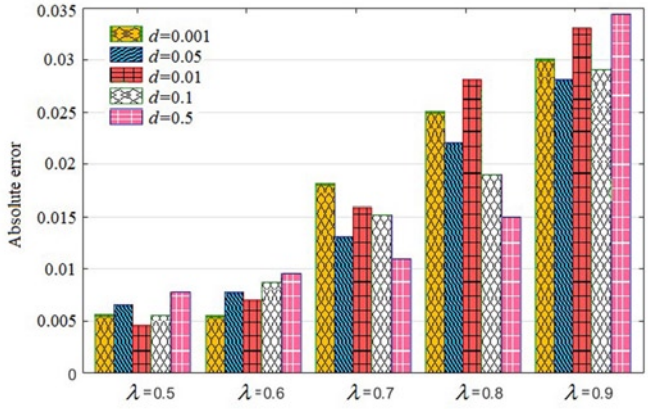

Fig. 8. Absolute error of optimization results under different parameter combinations

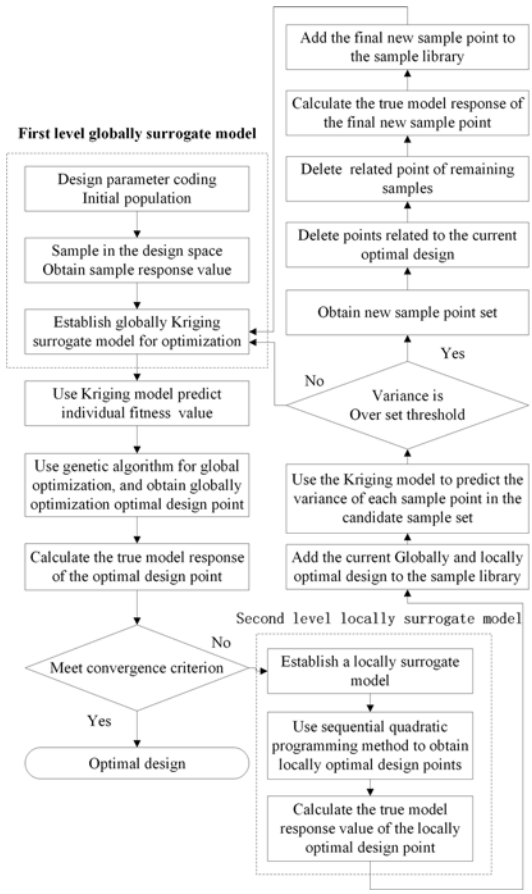

Fig. 9. Optimization flowchart for multi-level target agent

4. Multi-level Objective Surrogate Optimization Method

According to the genetic-algorithm-based Kriging surrogate model multi-point addition sequence optimization method proposed in section 3, the globality of optimization is strengthened by the choice of surrogate model, multi-point addition strategy and optimization algorithm. But this method does not consider the performance of the local search. In order to improve it, a multi-level surrogate model worked by global and local surrogate is presented. The flow chart of the multi-level surrogate model is shown in Fig. 9.

The first-level surrogate model is the Kriging globally surrogate model, the second-level surrogate model is the locally surrogate model. The detailed process is as follows. First, the genetic algorithm is used to optimize the Kriging globally surrogate model and obtain the globally optimal design points. Second, judge whether the convergence criterion is satisfied. If it is not satisfied, a locally surrogate model is established near the globally optimal design point (within 3σ), and the locally optimal design point of this iteration is obtained by the sequential quadratic programming method. Third, put the current globally, locally optimal design point and the real response into the sample library. Finally, delete the related point, and update the Kriging globally surrogate model until the convergence criterion is satisfied.

The locally surrogate model needs to have good local approximation ability to fit the objective function with high accuracy in a small design space. Quadratic PRS model and RBF model are both suitable for local fitting. The quadratic PRS model includes quadratic polynomial (QP) without cross terms and perfect quadratic polynomial (PQP) with cross terms [14, 3]. In order to select a more suitable locally surrogate model, three locally surrogate models are reconstructed. Three types of multi-level surrogate model are analyzed by adopting

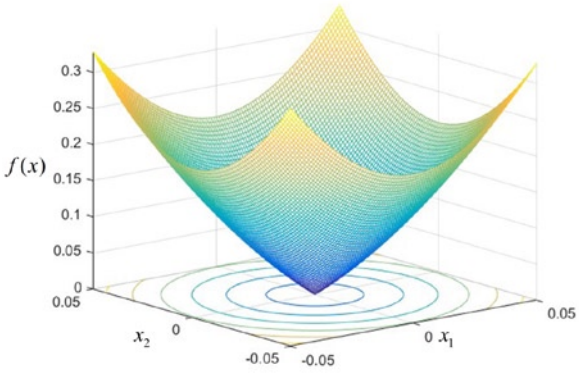

(a) Local surface graph of original function

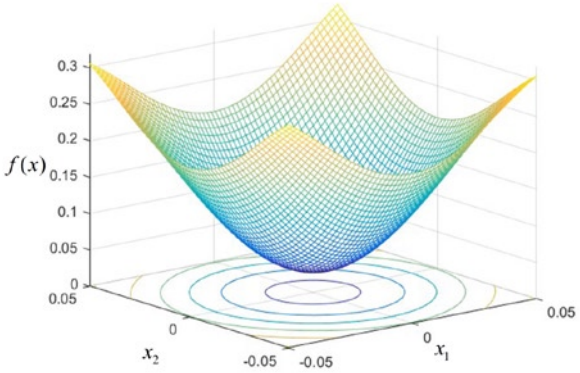

(b) PQP model

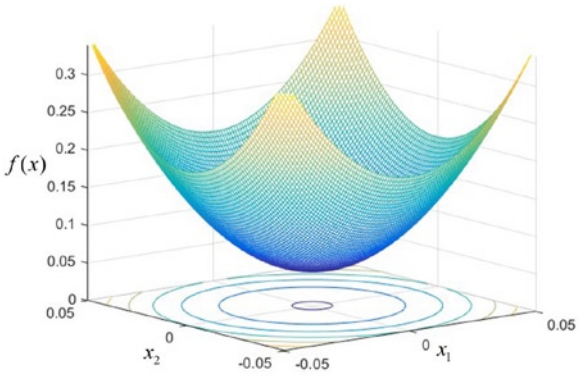

(c) QP model

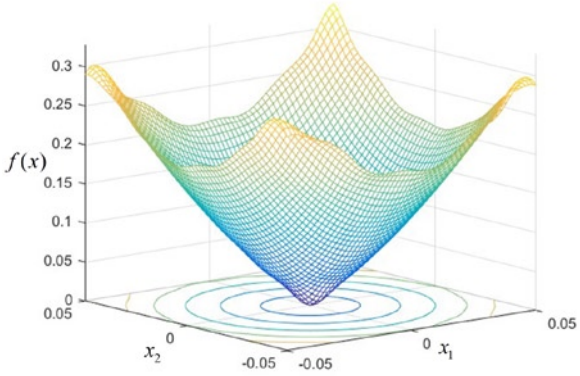

(d) RBF model

Fig. 10. Comparison of local surrogate model

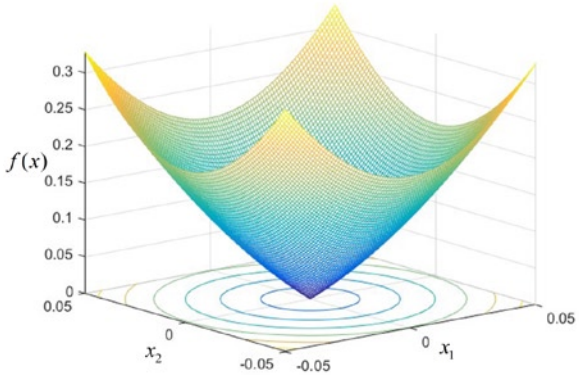

(a) Local surface graph of original function

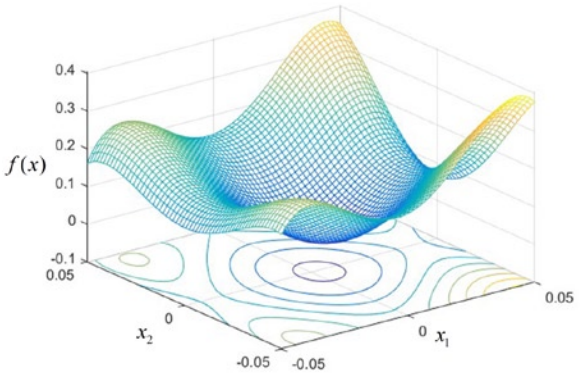

(b) PQP model

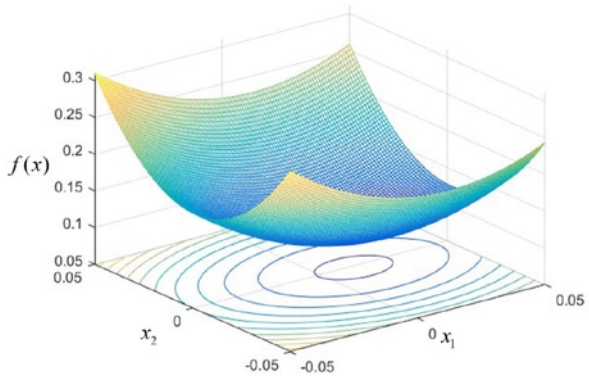

(c) QP model

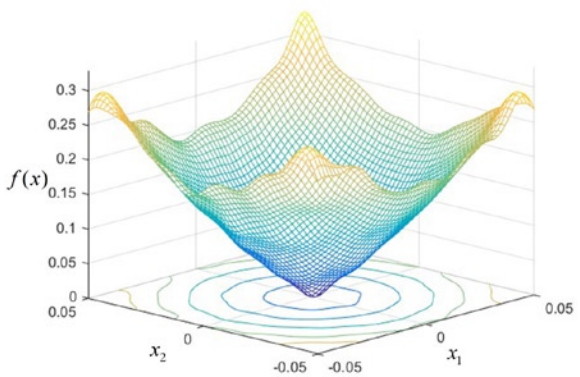

(d) RBF model

Fig. 11. Robustness comparison of the local surrogate model

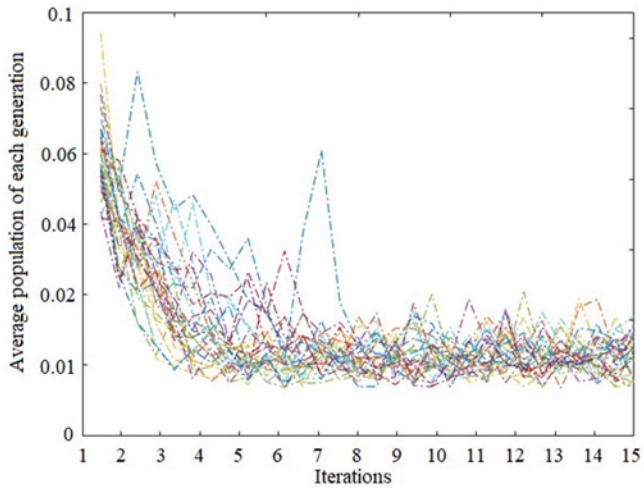

(a) Model I

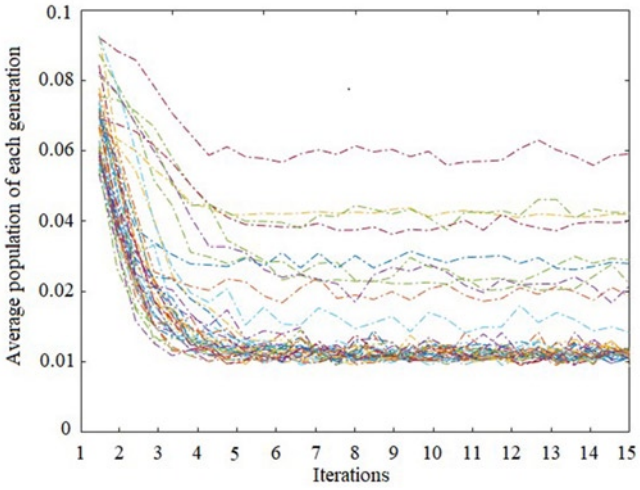

(b) Model II

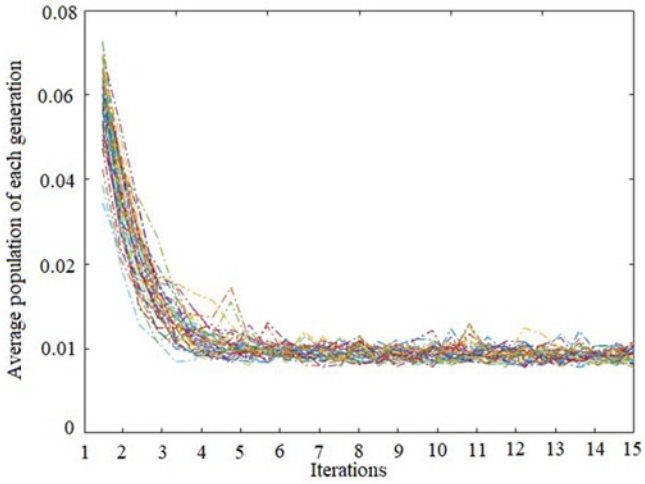

(c) Model III

Fig. 12. Robustness comparison of optimization algorithm

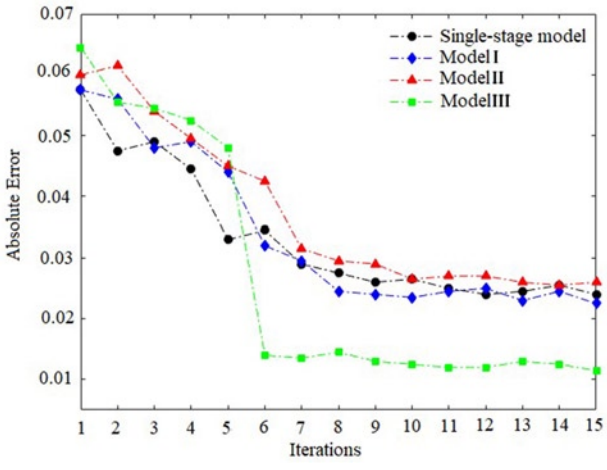

(a) RMSE

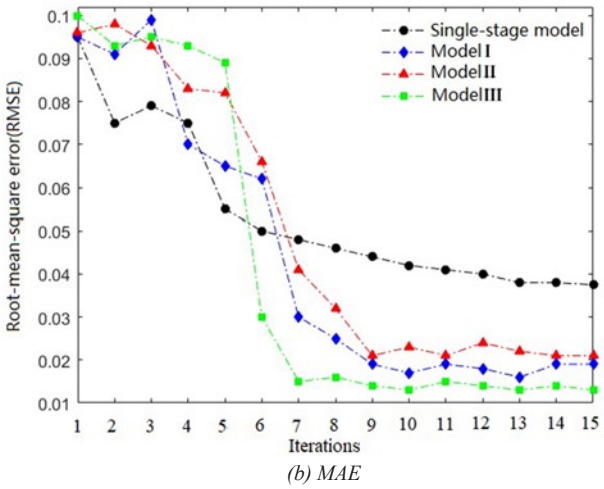

(b) MAE

Fig. 13. The change of the accuracy of the predicted optimal solution during the iterative process

the multi-level surrogate-based multi-point addition sequence optimization method. The three locally surrogate models are compared through the Ackley's Path test function.

Model I: the first-level globally surrogate model, Kriging model + the second-level locally surrogate model, PQP model;

Model II: the first-level globally surrogate model, Kriging model + the second-level locally surrogate model, QP model;

Model III: the first-level globally surrogate model, Kriging model + the second-level locally surrogate model, RBF model.

Fig. 10 shows the fitting surface of each local surrogate model at the true best point $f(0,0)=0$ when the optimization is terminated.

From Fig. 10 (a), it can be seen that due to the lack of nonlinear fitting ability of QP model, the fitted surface is quite different from the real one, and the fitting effect of PQP model is slightly better than that of QP model, but it still can't fit the surface accurately, which indicates that the quadratic PRS model can only simulate the overall trend. However, the response surface fitted by the RBF model is very close to the real response surface at the minimum peak value, and the fitting e0ffect is ideal.

In order to verify the robustness of the three local surrogate models, this paper adds Gaussian white noise with a signal-to-noise ratio of 1 to the test function. After adding noise, the fitted surfaces of each local surrogate model are shown in Fig. 11. From Fig. 11, it can be seen that the random noise has a significant effect on the fitting effect of the PQP model and the QP model, resulting in the surfaces fitted by these two models being completely distorted and deformed, which is very different from the real surface. However, the RBF model is less affected by random noise. Compared with the noise-free RBF model, although it is partially concave and convex, the two models are basically consistent on the whole, indicating that the RBF model has better robustness and is suitable for a local surrogate.

Fig. 12 shows the iteration curve obtained by performing 50 groups of design optimization for each local surrogate model. Each curve represents the average iterative history of each optimization from the initial population. Distribution and bandwidth of these curves can reflect the dependence on candidate sample groups of using different model optimizations. The distribution of the iterative curve of model I is messy; the bandwidth of model II is scattered, 8 lines are separated from the distribution concentration area; the bandwidth of model III is most uniform and narrow throughout the whole iteration process, and the average population can converge to 0.01 in each generation, which indicates that when using RBF as the local surrogate model the multi-level surrogate-based multi-point addition sequence optimization has the least dependence on the candidate sample group, and the optimization result is more accurate. From the above analysis, the RBF model is more suitable for the local surrogate model compared with the QP model and the PQP model.

In order to verify the advantages of the multi-level surrogate model, Fig. 13 shows the comparison of the absolute error average of the each generation optimal solutions for optimization designs of Ackley's Path test function. It can be seen from Fig. 13(a) that the single-level surrogate model and the multi-level surrogate model I~II require the average of 9 iterations and converge within 3% error at the same time. The multi-level surrogate model III can converge to the same error with only 6 iterations and the error is within 2%, so that the higher solution accuracy is obtained. Fig. 13(b) shows the comparison of the RMSE obtained 50 groups of optimization results. The single-level surrogate model converges slowly, and the final convergence error is the largest. The RMSE error fluctuations of the last few iterations of the multi-level surrogate models I and II are more obvious, the error is close to 2% after the iteration; the multi-level surrogate model III only needs 7 iterations to converge within 2%.

Through the above comparison, it is found that the multi-level surrogate model has faster convergence rate and higher accuracy. Therefore, this paper adopts the combination of globally Kriging surrogate and RBF locally surrogate to perform the reliability-based multi-level surrogate design optimization.

5. Multi-Level Surrogate Model Based Reliability Design Optimization Method

RBDO is a combination of reliability analysis and optimization design. It generally has two forms: one is to establish the mathematical model of reliability design optimization and seek its optimal solution with reliability as the constraint condition and cost, volume and mass as the optimization objective [29]; the other is to maximize the product reliability under the conditions that guarantee the certain performance and the economic indicators [10, 19].

Generally, RBDO with reliability as a constraint is more practical, and its mathematical model can be expressed as [13]:

$$\begin{aligned} &\text{Find} && x=(x_1,x_2,...,x_m)\\ &\text{Min} && f(x),\ x^L\le x\le x^U\\ &\text{s.t.} && P\left[g_j(x)>0\right]\ge[P_r]\\ &\text{or} && \beta_j(x)\ge[\beta] \end{aligned} \tag{8}$$

where m is the number of the random variables; x^U and x^L represent the upper and lower variable limits, $g(x)$ is the performance function; j is the number of performance functions corresponding to different failure forms; $[P_r]$ and $[\beta]$ represent specified reliability probability and reliability index design value.

In order to solve the problems that the actual objective function and structural performance function are difficult to obtain in the reliability optimization, the surrogate model technique is applied to approximate the objective function and the structural function. The method mentioned in section 4 is applied for optimization with the penalty function as reliability constraint. The construction process of the adaptive dynamic penalty function is as follows [4, 25]:

The objective satisfaction function and the constraint satisfaction function are applied. When there is a large difference between the objective function value and the penalty term, the general penalty function cannot effectively distinguish the feasible solution from the infeasible solution. The objective function $f(x)$ and the penalty term $p(x)$ are used to construct the function, respectively.

Objective constraint function:

$$\tilde{f}=\frac{f_{\max}-f(x)}{f_{\max}-f_{\min}}\in[0,1] \tag{9}$$

Constraint satisfaction function:

$$\tilde{p}=\frac{p_{\max}-p(x)}{p_{\max}-p_{\min}}\in[0,1] \tag{10}$$

where $f_{\max}$ and $f_{\min}$ are the maximum and minimum value of the objective function in the contemporary populations, $p_{\max}$ and $p_{\min}$ are the maximum and minimum of the penalty terms in the contemporary population. Obviously, they are both descending functions of the range $[0,1]$, which means $f(x)$ and $p(x)$ are inversely proportional to $\tilde{f}$ and $\tilde{p}$, respectively. Therefore, the individual's fitness is evaluated by objective satisfaction and constraint satisfaction. These two functions are employed to define a new penalty function $F(x)$:

$$F(x)=\begin{cases}\tilde{f}(x) & x\in D\\ \tilde{f}(x)+\tilde{p}(x)^{\alpha(1-\rho)\frac{2t-1}{t}} & x\notin D\end{cases} \tag{11}$$

where $r(\rho)=\alpha(1-\rho)[(2t-1)/t]$ is adaptive dynamic penalty factor; ρ is proportion of feasible solutions for contemporary populations; α is an integer parameter that needs to be adjusted of $[1,10]$; t is the evolution time.

The low-dimensional multi-constraint mathematical model is taken as a case to verify the feasibility of the method, which can be written as:

$$\begin{aligned}
&\text{Min} \quad f(x) = x_1 + x_2 \\
&\text{s.t.} \begin{cases}
P\left[g_j(x) > 0\right] \geq [P_r], \quad j = 1,2,3 \\
g_1 = x_1^2 x_2 / 20 - 1 \\
g_2 = (x_1 + x_2 - 5)^2 / 30 + (x_1 - x_2 - 12)^2 / 120 \\
g_3 = 80 / (x_1^2 + 8x_2 + 5) - 1 \\
0 \leq x_1, x_2 \leq 10 \\
[P_r] = 99.865\%
\end{cases}
\end{aligned} \tag{12}$$

where $g(x)$ is the structural performance function; x_1 and x_2 represent the independent variables: $x_1 \sim N(3.1, 0.3^2)$, $x_2 \sim N(2.09, 0.3^2)$.

The RBDO based on multi-level surrogate agent is taken as the scheme I, and the schemes II and III are also applied at the same time to be compared and analyzed. The three schemes are written as:

Scheme I: Multi-level objective surrogate + improved Kriging response surface method based on double-point addition;

Scheme II: Single-level objective surrogate + improved Kriging response surface method based on double-point addition;

Scheme III: Multi-level objective surrogate + Kriging response surface method.

The local surrogate model in the multi-level objective surrogate is RBF model. The relevant parameters are set as $\lambda = 0.7$, $d = 0.01$. The candidate sample sets number is 100, the number of population is 20, the selective probability is $p_c = 0.95$, the mutation probability is $p_m = 0.001$, the convergence precision is $\varepsilon = 0.001$. This method uses 15 uniform design points to do initial sampling of the objective function and performance function. The initial sample points are shown in Table 3.

The contour curve of the objective function, the constraint boundary of the performance function, and the real optimal solution are shown in Fig. 14(a). The real optimal solution satisfying the reliability constraint is $(3.439, 3.286)$, and its corresponding objective function value is 6.725. It can be seen from Fig. 14(b) and Fig. 14(c) that the g_1 and g_2 fitted by the Kriging model with two-point addition strategy is very good. Because of the nonlinearity of g_3 is the strongest, the fitting error is slightly larger in $[0, 2]$. Fig. 14(d) shows the fitting results of the general Kriging surrogate model, it can be seen that the general Kriging surrogate model has larger deviation from the fitting of g_2 and g_3.

The optimization results are shown in Table 4. From Table 4, N_{Obj} is the objective function running times, N_g is the performance function calculating times, $N = N_{Obj} + N_g$ is the total calculation cost. It can also be seen from Table 4 that the optimization results of the schemes I and II both meet the reliability constraint and the obtained reliability values have higher calculation accuracy. The optimal solution of the scheme I is slightly better than the scheme II. In terms of cost, function calculation costs of the scheme I has 59 times shorter than the scheme II. For the scheme III, the computation cost is too high and due to the poor reliability accuracy results of P_{r1} and P_{r2} is less than the value of the specified design $[P_r] = 99.865\%$. So the optimal solution does not meet the reliability constraint.

Fig. 15 shows the optimal solution iteration and the feasible solution proportion of each generation for each scheme. According to the trend of iteration, it can be seen that the small proportion of feasible solutions in the initial iteration ensures the diversity of the population. With the gradual increase of iterative evolution, mo−−−re feasible solutions enter the population. At the end of the iteration, the increase of feasible solutions slows down and tends to be stable. This evolution process is reasonable, and it also verifies the effectiveness of adaptive penalty function in dealing with reliability constraints.

In general, for the objective function optimization and reliability calculation, through the multi-level objective agent optimization method and the improved reliability algorithm proposed in this paper, the calculation cost can be reduced and the optimal solution obtained

Table 3. Initial sample points

Number	x_1	x_2	g_1	g_2	g_3	f_{Obj}
1	2.142	9.285	1.131	3.431	−0.046	11.428
2	5.000	8.571	9.714	3.469	−0.188	13.571
3	7.857	7.857	23.252	4.026	−0.382	15.714
4	0	7.142	−1.000	2.206	0.287	7.142
5	2.857	6.428	1.623	1.632	0.238	9.285
6	5.714	5.714	8.329	1.577	−0.040	11.428
7	8.571	5.000	17.367	2.041	−0.324	13.571
8	0.714	4.285	−0.890	1.020	1.010	5.000
9	3.571	3.571	1.277	0.353	0.726	7.142
10	6.428	2.857	4.903	0.204	0.156	9.285
11	9.285	2.142	8.238	0.574	−0.261	11.428
12	1.428	1.428	−0.854	0.353	3.331	2.857
13	4.285	0.714	−0.344	−0.408	1.750	5.000
14	7.142	0	−1.000	−0.650	0.428	7.142
15	10.000	10.000	49.000	7.700	-0.567	20.000

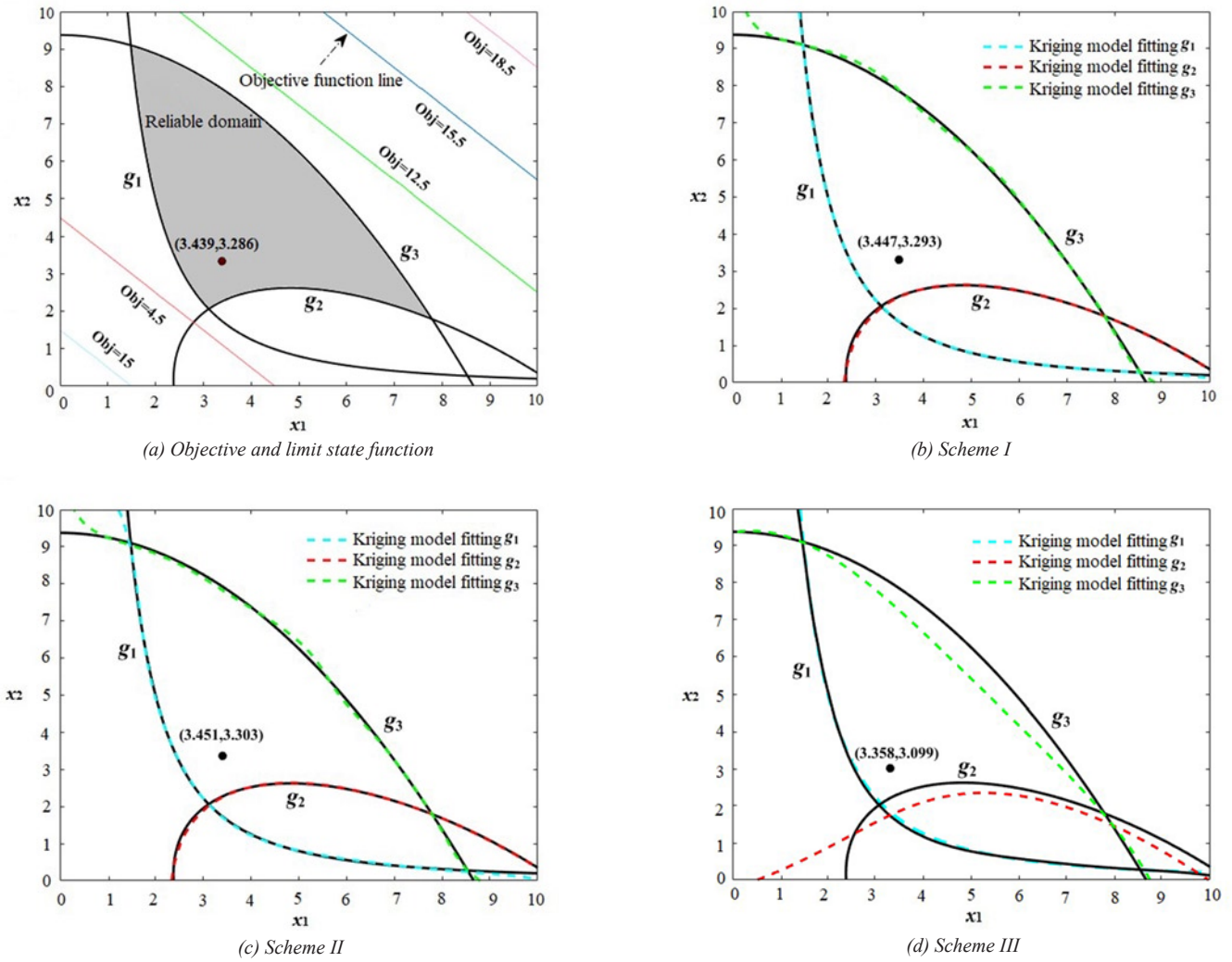

(a) Objective and limit state function

(b) Scheme I

(c) Scheme II

(d) Scheme III

Fig. 14. The approximate solution of reliability optimization under schemes I~III

Table 4. Results of RBDO

Scheme	Iteration times	Calculation cost	Optimal solution	Reliability	MC test	relative error %
I	4	N_{Obj} =57	x_1 =3.447	P_{r1} =0.99872	P_{r1} =0.99883	0.011
		N_g =175	x_2 =3.293	P_{r2} =0.99876	P_{r2} =0.99895	0.019
		N =232	f_{Obj} =6.740	P_{r3} =1.00000	P_{r3} =1.00000	–
II	6	N_{Obj} =77	x_1 =3.451	P_{r1} =0.99926	P_{r1} =0.99880	0.046
		N_g =214	x_2 =3.303	P_{r2} =0.99965	P_{r2} =0.99907	0.058
		N =291	f_{Obj} =6.754	P_{r3} =1.00000	P_{r3} =1.00000	–
III	5	N_{Obj} =62	x_1 =3.358	P_{r1} =0.98324	P_{r1} =0.99531	1.213
		N_g =2950	x_2 =3.099	P_{r2} =0.98933	P_{r2} =0.99808	0.877
		N =3012	f_{Obj} =6.457	P_{r3} =1.00000	P_{r3} =1.00000	–

can be ensured to be feasible. The scheme II adopts the single-level target surrogate mode. From the analysis results of the examples, it can be seen that the quality of the optimal solution and the calculation cost are worse than scheme I. In scheme III, the general Kriging surrogate model is used to calculate the reliability, resulting in a sharp increase in the number of calculation of the performance function. Moreover, due to the low accuracy of the reliability algorithm, the optimal solution cannot meet all the constraints.

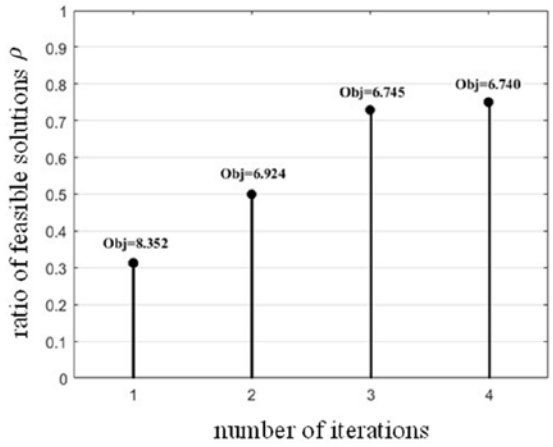

(a) Scheme I

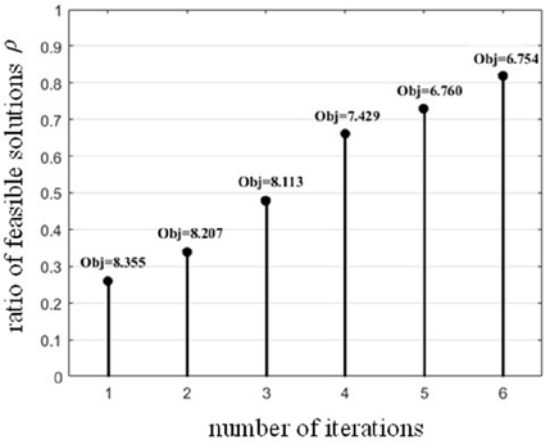

(b) Scheme II

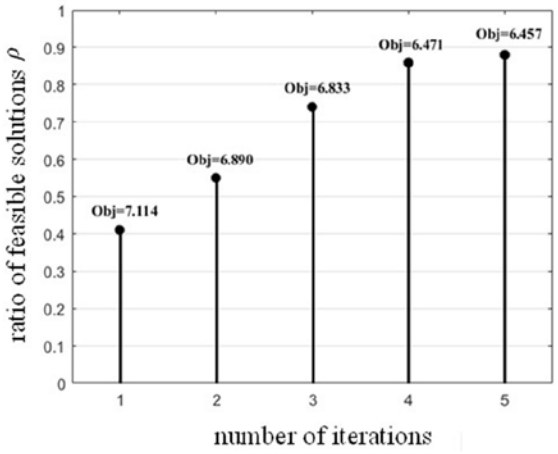

(c) Scheme III

Fig. 15. The optimal solution and the feasible solution ratio for each generation

6. Conclusions

In this work, a genetic-algorithm-based Kriging model using multi-point addition sequence optimization strategy is presented for the shortcomings of single point criterion in Kriging model sequence optimization. The local surrogate model is employed to modify the Kriging global surrogate model because of the poor local search performance of Kriging model, which proposed the multi-level surrogate model. Finally, a reliability-based design optimization is study combined with multi-level surrogate model and adaptive dynamic penalty function. The proposed approach is not only conceptually more understandable and computationally much more convenient, accurate and efficient, but also has more application value comparing to the traditional method. The contributions of the research work presented in this paper can be summarized as follows.

(1) The multi-point addition criterion of genetic-algorithm-based Kriging model is studied. The parameter λ and d which determine the number of final new samples of Kriging model has an important effect to the accuracy of the surrogate model. A smaller λ means more sample points will be add to the sample database, which can improve the fitting accuracy of Kriging model. Besides, when λ takes different values, the influence of d is different. When $\lambda < 0.7$, d has little effect to the model accuracy. However, when $\lambda \geq 0.7$ there is a great influence of d on the model accuracy.

(2) It is the first time that a Kriging-based multi-level surrogate model is first proposed, and its better convergence and accuracy is verified by with the example of Ackley's Path test function compared with PQP and QP model.

(3) A multi-level surrogate model based reliability design optimization method is provided and employed to solve a low-dimensional multi-constraint mathematical model. The case study results show that this method in consideration of the computation accuracy and efficiency simultaneously, thus avoiding the problem of slow convergence caused by the poor search ability of traditional methods.

Acknowledgement

This work was supported in part by the National Natural Science Foundation of China under Contract 51875073, in part by the Scientific Research Project of Education Department of Liaoning Province under Contract JDL2019005, in part by the Dalian Science and Technology Innovation Fund Plan under Contract 2019J11CY017, and in part by the Innovation Team Support Plan of Liaoning Higher Education under Contract LT2016010.

References

1. Ahmadi B, Nariman-zadeh N, Jamali A. Path synthesis of four-bar mechanisms using synergy of polynomial neural network and Stackelberg game theory. Engineering Optimization 2016; 49(6): 932–947, https://doi.org/10.1080/0305215X.2016.1218641.
2. Anuj K, Sangeeta P, Mangey R. System reliability optimization using gray wolf optimizer algorithm. Quality and Reliability Engineering

International 2017; 33(7): 1327-1335, https://doi.org/10.1002/qre.2107.
3. Buchheim C, Kurtz J. Robust combinatorial optimization under convex and discrete cost uncertainty. EURO Journal on Computational Optimization 2018; 6: 211–238, https://doi.org/10.1007/s13675-018-0103-0.
4. Chocat R, Beaucaire P, Debeugny L, Lefebvre J P, Sainvitu C, Breitkopf P, Wyart E. Damage tolerance reliability analysis combining Kriging regression and support vector machine classification. Engineering Fracture Mechanics 2019; 216: 1–13, https://doi.org/10.1016/j.engfracmech.2019.106514.
5. Di Somma M, Yan B, Bianco N, Graditi G, Luh P B, Mongibello L, Naso V. Multi-objective design optimization of distributed energy systems through cost and energy assessments. Applied Energy 2017, 204, 1299–1316, https://doi.org/10.1016/j.cma.2016.10.048.
6. Emre D, Ali R Y. A new hybrid approach for reliability-based design optimization of structural components. Materials Testing 2019; 61(2): 111–119, https://doi.org/10.3139/120.111291.
7. Freier L, Wiechert W, Von Lieres E. Kriging with trend functions nonlinear in their parameters: theory and application in enzyme kinetics. Engineering in Life Sciences 2017; 17(8): 1–10, https://doi.org/10.1002/elsc.201700022.
8. Gao H F, Wang A, Zio E, Ma W. Fatigue strength reliability assessment of turbo-fan blades by Kriging-based distributed collaborative response surface method. Eksploatacja i Niezawodnosc – Maintenance and Reliability 2019; 21(3): 530–538, https://doi.org/10.17531/ein.2019.3.20.
9. Gaspar B, Teixeira A P, Guedes Soares C. Adaptive surrogate model with active refinement combining Kriging and a trust region method. Reliability Engineering & System Safety 2017; 165: 277–291, https://doi.org/10.1016/j.ress.2017.03.035.
10. Haeri A, Fadaee M J. Efficient reliability analysis of laminated composites using advanced Kriging surrogate model. Composite Structures 2016; 149: 26–32, https://doi.org/10.1016/j.compstruct.2016.04.013.
11. Hawchar L, Soueidy C P E, Schoefs F. Global kriging surrogate modeling for general time-variant reliability-based design optimization problems. Structural and Multidisciplinary Optimization 2018; 58(3): 955–968, https://doi.org/10.1007/s00158-018-1938-y.
12. Heidari A A, Faris H, Aljarah I, Mirjalili S. An efficient hybrid multilayer perceptron neural network with grasshopper optimization. Soft Computing 2018; 23: 7941–7958, https://doi.org/10.1007/s00500-018-3424-2.
13. Ismail H Y, Singh M, Darwish S, Kuhs M, Shirazian S, Croker D M. Developing ANN-Kriging hybrid model based on process parameters for prediction of mean residence time distribution in twin-screw wet granulation. Powder Technology 2019; 343: 568–577, https://doi.org/10.1016/j.powtec.2018.11.060.
14. Korta J A, Mundo D. Multi-objective micro-geometry optimization of gear tooth supported by response surface methodology. Mechanism & Machine Theory 2017; 109: 278–295, https://doi.org/10.1016/j.mechmachtheory.2016.11.015.
15. Lara H, Charbel-Pierre E S, Franck S. Principal component analysis and polynomial chaos expansion for time-variant reliability problems. Reliability Engineering & System Safety 2017; 167: 406–416, https://doi.org/10.1016/j.ress.2017.06.024.
16.Li Y F, Huang H Z, Mi J, Peng W, Han X. Reliability analysis of multi-state systems with common cause failures based on Bayesian network and fuzzy probability. Annals of Operations Research 2019; https://doi.org/10.1007/s10479-019-03247-6.
17.Li Y H, Hu M G, Wang F. Fatigue life analysis based on six sigma robust optimization for pantograph collector head support. Advances in Mechanical Engineering 2016; 8(11): 1–9, https://doi.org/10.1177/1687814016679314.
18.Li Y H, Li Y H, Wang Y D, Wang J. Structural optimization–based fatigue durability analysis of electric multiple units cowcatcher. Advances in Mechanical Engineering 2017; 9(8): 1–10, https://doi.org/10.1177/1687814017726294.
19. Martínez-Frutos J, Herrero-Pérez D. Kriging-based infill sampling criterion for constraint handling in multi-objective optimization. Journal of Global Optimization 2015; 64(1): 97–115, https://doi.org/10.1007/s10898-015-0370-8.
20. Mi J H, Li Y F, Yang Y J, Peng W W, Huang H Z. Reliability assessment of complex electromechanical systems under epistemic uncertainty. Reliability Engineering & System Safety 2016; 152: 1–15, https://doi.org/10.1016/j.ress.2016.02.003.
21. Mi J, Beer M, Li Y F, Broggi M, Cheng Y. Reliability and importance analysis of uncertain system with common cause failures based on survival signature. Reliability Engineering & System Safety 2020; 106988, https://doi.org/10.1016/j.ress.2020.106988.
22.Narayanakumar S, Raja, K. A BP artificial neural network model for earthquake magnitude prediction in himalayas. Circuits and Systems 2016; 7: 3456–3468, https://doi.org/10.4236/cs.2016.711294.
23. Ozcanan S, Atahan A O. RBF surrogate model and EN1317 collision safety-based optimization of two guardrails. Structural and Multidisciplinary Optimization 2019; 60: 343–362, https://doi.org/10.1007/s00158-019-02203-z.
24. Stern R E, Song J, Work D B. Accelerated Monte Carlo system reliability analysis through machine-learning-based surrogate models of network connectivity. Reliability Engineering & System Safety 2017; 164: 1–9, https://doi.org/10.1016/j.ress.2017.01.021.
25. Sundar V S, Shields M D. Surrogate-enhanced stochastic search algorithms to identify implicitly defined functions for reliability analysis. Structural Safety 2016; 62: 1–11, https://doi.org/10.1016/j.strusafe.2016.05.001.
26. Vatteri A P, Balaji Rao, K, Bharathan, A M. Time-variant reliability analysis of RC bridge girders subjected to corrosion-shear limit state. Structural Concrete, 2016; 17(2), 162–174, https://doi.org/10.1002/suco.201500081.
27. Yadav R N. A hybrid approach of Taguchi-response surface methodology for modeling and optimization of duplex turning process. Measurement 2017; 100: 131–138, https://doi.org/10.1016/j.measurement.2016.12.060.
28. Yu J T. Research on wing design based on reliability optimization. Shenyang Aerospace University, 2015.
29. Yu S, Wang Z L, Zhang K W. Sequential time-dependent reliability analysis for the lower extremity exoskeleton under uncertainty. Reliability Engineering and System Safety 2018; 170: 45–52, https://doi.org/10.1016/j.ress.2017.10.006.
30. Zhang Y, Lin F Y. Optimum design of collision reliability of aluminum foam filled thin wall structure. Journal of Mechanical Engineering 2011; 47(22): 93–99, https://doi.org/ 10.3901/JME.2011.22.093.
31. Zhi P P, Li Y H, Chen B Z, Li M, Liu G N. Fuzzy optimization design-based multi-level response surface of bogie frame. International Journal of Structural Integrity 2019; 10(2): 134–148, https://doi.org/10.1108/IJSI-10-2018-0062.
32. Zhou W, Fang J. Application of improved response surface method in reliability optimization of body tubes. Mechanical Science and Technology 2016; 2: 176–181, https://doi.org/10.13433/j.cnki.1003-8728.2016.0203.
33. Zhu L, Zhang Y, Zhang R, Zhang P. Time-dependent reliability of spur gear system based on gradually wear process. Eksploatacja i Niezawodnosc – Maintenance and Reliability 2018; 20 (2): 207–218, https://doi.org/10.17531/ein.2018.2.05.
34. Zhu S P, Huang H Z, Peng W, Wang H K, Sankaran M. Probabilistic Physics of failure-based framework for fatigue life prediction of aircraft gas turbine discs under uncertainty. Reliability Engineering & System Safety 2016; 146: 1–12, https://doi.org/10.1016/j.ress.2015.10.002.